

# T-MATRIX DE-EMBEDDING OF IC METAL TRANSMISSION LINES TO 18 GHz

Timothy J. Maloney and Quat T. Vu  
Intel Corporation  
Santa Clara, CA 95052

## ABSTRACT

T-matrix methods are applied to S-parameter data from on-chip metal lines connected to microwave measurement equipment so as to preserve mirror symmetry in the entire system. The propagation constant  $\gamma$  and characteristic impedance  $Z_{in}$  of a line are derived from measurements on two different lengths of line. It is shown here that  $Z_{in}$  can be found with few assumptions about the transition networks. In particular, we present a theorem for determining  $Z_{in}$  or its phase for any symmetric or lossless transition network. Multiple lengths of otherwise identical IC line allow redundant, pairwise solutions to be acquired, with high confidence in the final result. Experimental results show that today's IC metal lines at Intel can have flat R, L, G, and C to at least 18 GHz.

## I. INTRODUCTION

Integrated circuits of the year 2000 will require the knowledge of IC metal transmission line circuit parameters R, L, G, and C to very high frequency, in order to allow for sharp signal edge design. These parameters can be derived from two complex numbers, the propagation constant  $\gamma$  and the impedance  $Z_{in}$ .

In this work, T-matrix methods are applied to on-chip metal lines having transition networks (also known as port discontinuities) to microwave measurement equipment which are identical on either side; i.e., there is an axis of symmetry in the center of the line which is easily checked by confirming that  $S_{11}=S_{22}$  for the entire system.

The transmission matrix de-embedding methods developed herein are used to extract propagation constant  $\gamma$  and impedance  $Z_{in}$  for on-chip lines as

shown in Figure 1, which interfaced to microwave measurement equipment through symmetric transition networks. The T-matrix approach was initiated in response to a need to characterize a particular set of IC transmission line test structures. Y-matrix de-embedding techniques [1-3] proved inadequate because of the inherent assumption that transition networks behave like lumped admittances at all frequencies; also there were not a wealth of "dummy" structures to allow complete pad characterizations in the absence of a line.

## II. PROPAGATION CONSTANT

Suppose we have S-parameter data for two lengths of on-chip transmission line as in Figure 1, each line being identical except for the length of the segment (B) connecting the two mirror-symmetric transitions (A and C). If  $l$  is the difference between the two line lengths, then we can consider Network 2 (with the longer line) to be like Network 1 but with line length  $l$  inserted into the middle. Given that [4] the T-matrix of a transmission line  $l$  is

$$T_{line} = \begin{bmatrix} e^{-\gamma l} & 0 \\ 0 & e^{+\gamma l} \end{bmatrix},$$

the T-matrices for Networks 1 and 2 can be written as follows:

$$T_1 = \begin{bmatrix} a & b \\ c & d \end{bmatrix} \begin{bmatrix} a & -c \\ -b & d \end{bmatrix} = \begin{bmatrix} K_1 & K_2 \\ K_3 & K_4 \end{bmatrix},$$

$$T_2 = \begin{bmatrix} a & b \\ c & d \end{bmatrix} \begin{bmatrix} e^{-\gamma l} & 0 \\ 0 & e^{+\gamma l} \end{bmatrix} \begin{bmatrix} a & -c \\ -b & d \end{bmatrix} = \begin{bmatrix} U_1 & U_2 \\ U_3 & U_4 \end{bmatrix}$$

[Eqs. 1]

From these it has been shown in several works [5,6] that the propagation constant is found in the solution to a quadratic equation:

$$x = e^{\gamma l} = \frac{2U_2K_2 + K_1U_4 + U_1K_4 \pm \sqrt{(2U_2K_2 + K_1U_4 + U_1K_4)^2 - 4}}{2}. \quad [\text{Eq. 2}]$$

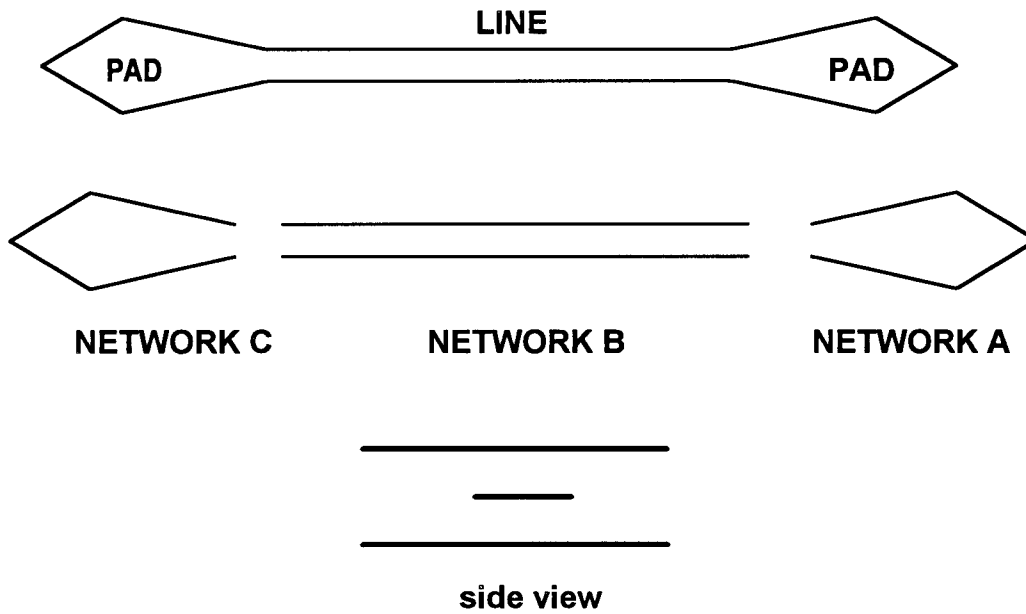


Figure 1. Embedded T-line and pad transitions, showing mirror symmetry and cross section.

The two values for  $x$  (one choice obvious for a passive, dissipative network) can also be obtained as the eigenvalues of a matrix  $(=T_2 \cdot (T_1)^{-1})$  derivable from the measured  $T_1$  and  $T_2$  matrices [7]. In the next section, the eigenvectors of  $T_2 \cdot (T_1)^{-1}$  help us to find the line impedance  $Z_{in}$ .

### III. IMPEDANCE

The key to finding the impedance  $Z_{in}$  of the embedded line is that the interior matrix of the lines "wxyz" between the symmetric transition networks

$$T_{1,2} = \begin{bmatrix} a & b \\ c & d \end{bmatrix} \begin{bmatrix} w & x \\ y & z \end{bmatrix} \begin{bmatrix} a & -c \\ -b & d \end{bmatrix}, \text{ [Eqs. 3]}$$

is derived from a transformed normalized line as in Figure 2.

Once the turns ratio  $n$  is determined, the T-line's  $Z_{in}$  is found to be  $Z_0 n^2$  or  $50n^2$ . Using transformer T-matrices from [4], the T-matrix of the network in Figure 2 is

$$\begin{bmatrix} w & x \\ y & z \end{bmatrix} = \begin{bmatrix} p & -q \\ -q & p \end{bmatrix} \begin{bmatrix} e^{-\gamma l} & 0 \\ 0 & e^{+\gamma l} \end{bmatrix} \begin{bmatrix} p & q \\ q & p \end{bmatrix}, \text{ [Eqs. 4]}$$

where

$$p = \frac{1}{2} \left( \frac{1}{n} + n \right), \quad q = \frac{1}{2} \left( \frac{1}{n} - n \right).$$

Note that  $p + q = \frac{1}{n}$ ,  $p - q = n$ ,  $p^2 - q^2 = 1$ ,

so  $p = \cosh \delta$ ,  $q = \sinh \delta$ . The transformer matrices thus depend on a single variable, traceable to  $n$ .

Substituting Eqs. 4 into Eqs. 3, we get the T-matrix of an embedded line of length  $l$ :

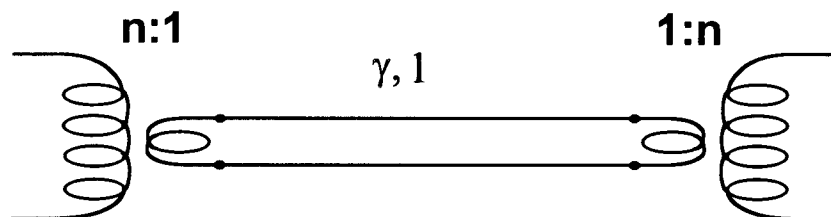


Figure 2. Circuit model of embedded T-line as seen from an external measurement system.

$$\mathbf{T} = e^{-\gamma l} \begin{bmatrix} T_1 & T_2 \\ T_3 & T_4 \end{bmatrix},$$

$$T_1 = a^2(p^2 - q^2 e^{+2\gamma l}) - 2abpq(1 - e^{+2\gamma l}) - b^2(p^2 e^{+2\gamma l} - q^2)$$

$$T_2 = -ac(p^2 - q^2 e^{+2\gamma l}) + (ad + cb)pq(1 - e^{+2\gamma l}) + db(p^2 e^{+2\gamma l} - q^2)$$

$$T_3 = ac(p^2 - q^2 e^{+2\gamma l}) + (ad + cb)pq(e^{+2\gamma l} - 1) - db(p^2 e^{+2\gamma l} - q^2)$$

$$T_4 = c^2(q^2 e^{+2\gamma l} - p^2) + 2cdpq(1 - e^{+2\gamma l}) + d^2(p^2 e^{+2\gamma l} - q^2)$$

[Eqs. 5]

The matrices  $\mathbf{T}_1$  and  $\mathbf{T}_2$  as described above are associated with line lengths  $l_1$  and  $l_2$ , respectively. Certain linear combinations of these two matrices reduce their complexity. If we take

$$\mathbf{A} = \frac{e^{\gamma l_1} \mathbf{T}_1 - e^{\gamma l_2} \mathbf{T}_2}{e^{2\gamma l_1} - e^{2\gamma l_2}}, \text{ and also}$$

$$\mathbf{C} = \frac{e^{-\gamma l_1} \mathbf{T}_1 - e^{-\gamma l_2} \mathbf{T}_2}{e^{-2\gamma l_1} - e^{-2\gamma l_2}}, \quad [\text{Eqs. 6}]$$

it eventually follows that

$$\begin{bmatrix} a & b \\ c & d \end{bmatrix} \begin{bmatrix} p & -q \\ -q & p \end{bmatrix} = \begin{bmatrix} \sqrt{C_{11}} & -\sqrt{-A_{11}} \\ \sqrt{-C_{22}} & -\sqrt{A_{22}} \end{bmatrix}. \quad [\text{Eqs. 7}]$$

This is an original way to express the particular solution to the eigenmatrix as discussed in [7]. The proper sign of the square roots can be selected with the help of the reciprocity relation  $\sqrt{-A_{11}}\sqrt{-C_{22}} - \sqrt{C_{11}}\sqrt{A_{22}} = 1$  and the mirror symmetry ( $S_{11}=S_{22}$ ) of the entire network. These equations can be manipulated to solve for  $\delta$  and therefore  $n^2$  and  $Z_{in}$  to give a universal expression relating to the impedance,

$$n^2 = \frac{C_+ - A_+}{C_- + A_-} \left[ \frac{a + d - b - c}{a + d + b + c} \right], \quad [\text{Eq. 8}]$$

where

$$A_{\pm} = \sqrt{-A_{11}} \pm \sqrt{A_{22}}, \quad C_{\pm} = \sqrt{-C_{11}} \pm \sqrt{C_{22}}.$$

Because Eqs. 7 are 4 equations in 5 unknowns, some constraint on the transition network is needed. For any internally symmetric transition network,  $b+c=0$ , and

$$n^2 = \frac{C_+ - A_+}{C_- + A_-}. \quad [\text{Eq. 9}]$$

Please note the distinction between the easily verified mirror symmetry of the entire system and the possible internal symmetry of the port discontinuity (transition network) on either side of the line.

In the case of a shunt-series-shunt Y'-Z-Y network (Fig. 3) for the transition, Eq. 8 becomes

$$n^2 = \frac{C_+ - A_+}{C_- + A_-} \left[ \frac{1 + ZY}{1 + ZY'} \right] \quad [\text{Eq. 10}]$$

after applying the T-matrix expressions in [4] for the Y and Z elements:

$$\mathbf{T}_Y = \begin{bmatrix} 1 - \frac{Y}{2} & -\frac{Y}{2} \\ \frac{Y}{2} & 1 + \frac{Y}{2} \end{bmatrix},$$

$$\mathbf{T}_Z = \begin{bmatrix} 1 - \frac{Z}{2} & \frac{Z}{2} \\ -\frac{Z}{2} & 1 + \frac{Z}{2} \end{bmatrix}.$$

Finally, for a lossless series-shunt transition network of any number of purely reactive Y-Z elements, it can be shown that

$$n^2 = \frac{C_+ - A_+}{C_- + A_-} \left[ \frac{\text{Re}(a) - \text{Re}(b)}{\text{Re}(a) + \text{Re}(b)} \right]. \quad [\text{Eq. 11}]$$

as a consequence of the fact that  $b=c^*$  and  $a=d^*$  for  $\mathbf{T}_Y$  and  $\mathbf{T}_Z$  (and such lossless elements as T-lines), properties that are retained for products of such matrices. Thus Eq. 11 applies to any ordinary lossless filter section or matching network.

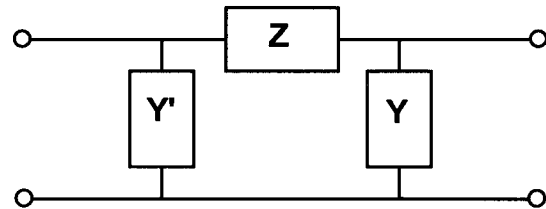


Figure 3. Pi network for transition, with series Z bridging shunt admittances.

The phase of the impedance or more can thus be determined for any symmetric or lossless transition network, a remarkable result. The phase of  $Z_{in}$  tells us immediately whether the embedded line has any losses through the G or R elements. Following from Marks and Williams

[8], we can see immediately if  $G \ll \omega C$  is correct over frequency by checking  $\gamma/Z_{in} = G + j\omega C$  to see if the phase of  $\gamma$  always leads that of  $Z_{in}$  by  $90^\circ$  to give  $\gamma/Z_{in} = j\omega C$ . If  $C$  is constant over the frequency range, as often expected, we have easy access to the full  $Z_{in}$ . In this way we check the dielectric properties of the transmission line, from losses to dielectric constant, over the frequency band. As [8] suggests, frequency dependence of  $R$  and  $L$  ought to occur more readily than it would for  $C$ .

At this point it is clear that a symmetric transition network gives an exact solution for  $Z_{in}$  and the problem is solved, while a lossless one will at least give the phase of  $Z_{in}$  and allow the capacitance to be investigated as described above. If we wish to make no assumptions about the line parameters  $G$ ,  $C$ ,  $R$  and  $L$  we need to assume something about the transition network because Eqs. 7 are underconstrained; numerous other authors have faced the same situation in de-embedding. The symmetric transition network is even allowed to have lossy or frequency-dependent components, a concept that has been used successfully by other authors in extracting balanced  $\pi$ -networks of microwave transitions [9,10]. Other work on microstrip impedance extraction [11] suggests that the transition can be taken to be reactive and electrically short, although not without some phase shift; such a transition is seen to be symmetric and lossless. It is thus reasonable to expect commercial microwave probes onto wide metal pads (see below) to agree with symmetric and/or lossless conditions so as to make Eqs. 9-11 very useful.

The net effect of Eqs. 9-11 is to allow impedance extraction based on a few general assumptions about the port discontinuities, without giving up the ability to check the dielectric constant for the behavior of its real and imaginary parts over frequency. If any unexpected variations in  $G$  or  $C$  are observed, Eqs. 9-11 give a framework in which to check whether the observation could be related to the transition networks themselves.

## IV. EXPERIMENT

The T-matrix de-embedding method described above was validated using a three metal level test structure consisting of aluminum lines of  $1.8\mu\text{m}$  wide,  $0.5\mu\text{m}$  thick on metal level 2, with ground planes on metal levels 1 and 3 as in Fig. 1. Line lengths of 1, 2, 4, 8 and 16mm were patterned.

The S-parameter setup consisted of the HP 8510B Vector Network Analyzer which covers the range of frequency from 50 MHz to 20 GHz. The Cascade Microtech on-chip probes of the GS type are valid up to 18 GHz. Mirror symmetry of these probes and their pads was assured through S-parameter measurement. The setup is controlled by computer through HP TECAP/ICCAP software, and the analysis was carried out using the ICCAP software.

For these test structures, we find the transmission line parameters  $R$ ,  $L$ ,  $G$ , and  $C$  to be flat to 18 GHz, with  $G \approx 0$  at all frequencies. Values of  $R$  match dc values, as our skin depth at 18 GHz is around  $0.7\mu\text{m}$ . Plots of these results have been published previously by the authors [12], showing the improvement over the Y-matrix method at high frequency. Once the algorithm was tested out on this stripline case of simple TEM waves, it was further used on other cases of interest, e.g., quasi-TEM or microstrip-like on-chip lines.

The transition networks were found to be symmetric and lossless in this work, and fit a C-L-C balanced  $\pi$ -network with approximate values of  $C=217\text{fF}$  on either side of  $L=100\text{pH}$ . These can be found from Eqs. 7 after finding the impedance and then solving for  $a, b, c$ , and  $d$  knowing  $\delta$ . In the Y-Z-Y model,

$$Z = \frac{b+d-a-c}{2}, YZ = a+d-1.$$

For low frequencies, where  $Z \approx 0$ , one just makes use of  $a=1-Y/2$  to solve for the total  $Y$ .

## V. DISCUSSION

This work was initiated in response to a need to characterize a particular set of IC transmission line test structures. Y-matrix de-embedding techniques proved inadequate because of the inherent assumption that transition networks behave like lumped admittances at all frequencies. Due to phase shifts at high frequency, this did not work because a series  $Z$  element was needed. Combining Y- and Z-matrix techniques would have been sufficient, but would have also required new dummy test structures to complete the analysis. Thus the T-matrix method was developed to solve the problem.

A significant feature of the T-matrix method is its freedom from "dummy" structures, although it requires at least two lengths. While for most

cases, dummy structures can be easily included in the test pattern, there are situations where the field configuration of the dummy pad under measurement is not similar to the field configuration when the pad is attached to the interconnect line. Such is the case when ground is not a large plane or planes.

A second feature of the T-matrix method is that the pad parasitics are extracted from the measurements of two line lengths. These parasitic values correspond to the true "running" situation. This is to be contrasted to the measurements of the pad parasitics when the pads are just dummies.

As evident from earlier discussions in this work, "Thru-Reflect-Line" (TRL) calibration techniques provide a most interesting connection to our de-embedding goals. The work of Soares, et. al. in 1989 [7] unifies the TRL theory in a rigorous mathematical way with matrix algebra, including an elegant proof that the propagation constant  $\gamma$  can be obtained from the eigenvalues of a matrix  $(=T_2 \cdot (T_1)^{-1})$  obtained from measurements on two lengths of line. The transition networks are a particular solution of the eigenvectors of that matrix. As discussed earlier, the propagation constant can be obtained irrespective of any symmetry in the transition network, as befits a calibration technique. This fact was known when the TRL method began a decade earlier [5], although at that time it was not recognized how useful it would be to diagonalize the measured matrix.

As discussed in [7], finding the correct particular solution of the 2x2 eigenmatrix requires two constants to be determined. One arises from the reciprocity condition, but the other must come from some kind of constraint on the two transition networks, usually a symmetry constraint. Ref. 7 shows how this can be done in several ways. Our use of full mirror symmetry in the transition networks was a little more than the absolute minimum needed, but it paid off for the goal of de-embedding IC lines, because everything self-checked for our structures. Also, the expressions in Eqs. 7-11 were more compact and useable than anything we obtained by trying to find the proper eigenmatrix.

It is interesting to compare the T-matrix techniques with another de-embedding algorithm by Rautio [13], which uses lines of length L and 2L, and matrix methods that remind one of [5]

and [7]. Indeed, the work can be seen in part as a special case of those TRL methods. But, from our point of view, requiring lengths L and 2L reduces the number of applicable test structures, and also reduces the ease of acquiring redundant data. Ref. 13 is especially interesting in its discussion of the difficulty of dealing with more than a shunt admittance in the equivalent circuit of the port discontinuity (transition network), and the difficulty of extracting the impedance of an embedded line.

Another paper shows how to characterize resistive embedded transmission lines by time-domain techniques using short pulses [14]. This method requires equipment very different from ours, however. An earlier paper from the same group [15] finds most of the frequency-dependent behavior of long metal lines to be due to skin depth effects. When the skin depth  $\delta$  becomes significantly small compared to the metal line dimensions, the transmission line parameters R and L are affected because current is confined to the outer skin depth of the metal. For our Al lines, with resistivity  $\rho$  about  $3 \mu\Omega\text{-cm}$ , our skin depth at 18 GHz is around  $0.7 \mu\text{m}$ . It is thus not surprising that our  $0.5 \mu\text{m}$  thick lines do not show resistive or inductive effects over the measured frequency range. Thicker lines would be needed to show the skin depth effects as expressed by  $\gamma Z_{in} = R + j\omega L$ , R and L now frequency-dependent.

## VI. SUMMARY

We have developed T-matrix methods for extraction of propagation constant and impedance of on-chip metal lines which allow a full investigation of the frequency-dependent properties of the lines with a minimum of assumptions about the transition networks (port discontinuities). While the propagation constant is generally accessible, as has long been known, we have shown that the phase of the impedance is known for a lossless pair of transitions, and the full impedance is known for an individually symmetric pair of transitions. These methods require a minimum of dummy structures and allow extraction of parameters from pairwise combinations of line length, which in turn allows cross-checking and greater freedom to use available test structures.

These T-matrix methods were ideally suited to our test structure set, and allowed us to satisfy our goal of a fundamental investigation of IC

metal line parameters at high frequency. The methods were uniquely capable of showing that today's IC metal lines at Intel can have flat R, L, G, and C to at least 18 Ghz.

## ACKNOWLEDGEMENT

The authors would like to thank Paul van Wijnen for his contributions to this work while he was at Intel.

## REFERENCES

1. P.J. van Wijnen, H.R. Claessen, and E.A. Wolsheimer, "A New Straightforward Calibration and Correction Procedure for On-Wafer High Frequency S-Parameter Measurements (45 MHz-18 GHz)", Proceedings of the Bipolar Circuits and Technology Meeting 1987, Minneapolis, Minnesota, pp. 70-73, Sept. 1987.
2. M.C.A.M. Koolen, J.A.M. Geelen and M.P.J.G. Versleijen, "An Improved De-embedding Technique for On-Wafer High Frequency Characterization", Proceedings of the Bipolar Circuits and Technology Meeting, 1991, pp. 188-191, September 1991.
3. H. Cho and D.E. Burk, "A Three-Step Method for the De-embedding of High-Frequency S-Parameter Measurements", IEEE Trans. on Electron Devices, ED-38, No.6, pp. 1371-1375, June 1991.
4. S. Ramo, J. Whinnery, and T. van Duzer, *Fields and Waves in Communication Electronics*, Wiley, 1965; see especially Sec. 11.09-11.11, pp. 603-612.
5. G.F. Engen, "'Thru-Reflect-Line': An Improved Technique for Calibrating the Dual Six-Port Automatic Network Analyzer", IEEE Trans. Microwave Theory Tech., MTT-27, pp. 987-993, Dec. 1979.
6. J.P. Mondal and T-H. Chen, "Propagation Constant Determination in Microwave Fixture De-Embedding Procedure", IEEE Trans. Microwave Theory Tech., MTT-36, pp. 706-714, Apr. 1988.
7. R.A. Soares, P. Gouzien, P. Legaud, and G. Follot, "A Unified Mathematical Approach to Two-Port Calibration Techniques and Some Applications", IEEE Trans. Microwave Theory Tech., MTT-37, pp. 1669-1673, Nov. 1989.
8. R.B. Marks and D.F. Williams, "Characteristic Impedance Determination Using Propagation Constant Measurement", IEEE Microwave and Guided Wave Letters 1, pp. 141-143 (1991).
9. J.S. Kasten, M.B. Steer, and R. Pomerleau, "Enhanced Through-reflect-Line Characterization of Two-Port Measuring Systems Using Free-Space Capacitance Calculation", IEEE Trans. Microwave Theory Tech., MTT-38, pp. 215-217, Feb. 1990.
10. S.B. Goldberg, M.B. Steer, P. D. Franzon, and J.S. Kasten, "Experimental Electrical Characterization of Interconnects and Discontinuities in High-Speed Digital Systems", IEEE Trans. on Components, Hybrids, and Manufacturing Technology, CPMT-14, pp. 761-765, Dec. 1991.
11. W.J. Getsinger, "Measurement and Modeling of the Apparent Characteristic Impedance of Microstrip", IEEE Trans. Microwave Theory Tech., MTT-31, pp. 1669-1673, Aug. 1983.
12. Q. T. Vu, P. J. van Wijnen, and T. J. Maloney, "High Speed Sub-Half-Micron Interconnect Characterization up to 18 GHz", VLSI Multilevel Interconnection Conference, June 1994.
13. J.C. Rautio, "A De-Embedding Algorithm for Electromagnetics", International Journal of Microwave and Millimeter-Wave Computer-Aided Engineering, 1, pp. 282-287 (1991).
14. A. Deutsch, G. Arjavalingham, and G.V. Kopcsay, "Characterization of Resistive Transmission Lines by Short-Pulse Propagation", IEEE Microwave and Guided Wave Letters 2, pp. 25-27 (1992).
15. A. Deutsch, G.V. Kopcsay, and 11 others, "High-Speed Signal Propagation on Lossy Transmission Lines", IBM J. Res. Develop. 34, 601-615, July 1990.